C. R. Physique 15 (2014) 224–240

Contents lists available at ScienceDirect

Comptes Rendus Physique

www.sciencedirect.com

Electron microscopy / Microscopie électronique

In situ mechanical TEM: Seeing and measuring under stress with electrons

Voir et mesurer sous contrainte mécanique avec des électrons : La microscopie électronique à transmission (MET) in situ

Marc Legros

CEMES–CNRS, 29, rue Jeanne-Marvig, 31055 Toulouse, France

ARTICLE INFO

Article history:
Available online 5 March 2014

Keywords:
In situ TEM
Plastic deformation
Dislocation structure and dynamics

Mots-clés :
Microscopie MET in situ
Déformation plastique
Structure et dynamique des dislocations

ABSTRACT

From the first observation of moving dislocations in 1956 to the latest developments of piezo-actuated sample holders and direct electron sensing cameras in modern transmission electron microscopes (TEM), in situ mechanical testing has brought an unequaled view of the involved mechanisms during the plastic deformation of materials. Although MEMS-based or load-cell equipped holders provide an almost direct measure of these quantities, deriving stress and strain from in situ TEM experiments has an extensive history. Nowadays, the realization of a complete mechanical test while observing the evolution of a dislocation structure is possible, and it constitutes the perfect combination to explore size effects in plasticity. New cameras, data acquisition rates and intrinsic image-related techniques, such as holography, should extend the efficiency and capabilities of in situ deformation inside a TEM.

RÉSUMÉ

Des premières observations du mouvement de dislocations en 1956 jusqu'aux derniers développements de porte-objets à commandes piézo-électriques et de caméras à détection d'électrons dans les microscopes électroniques à transmission (MET) modernes, les essais mécaniques in situ ont toujours permis une observation inégalée des mécanismes impliqués dans la déformation plastique. Bien que les porte-objets équipés d'une cellule de charge ou de MEMS offrent une visualisation presque directe de ces effets, l'élaboration des étapes nécessaires pour mesurer les relations entre contrainte et déformation à partir d'expériences réalisées in situ dans un MET a une longue histoire. Aujourd'hui, la réalisation d'un essai mécanique complet tout en observant l'évolution d'une structure de dislocations est possible ; ceci constitue la combinaison parfaite pour explorer les effets de taille dans la plasticité. Les nouvelles techniques intrinsèques d'imagerie (comme l'holographie en champ sombre) et l'accès à de nouveaux outils d'acquisition d'images (nouvelles caméras, taux d'acquisition rapides) vont étendre l'efficacité et les capacités de mesures sans entraver l'observation des mécanismes.

http://dx.doi.org/10.1016/j.crhy.2014.02.002
1631-0705/

1. Introduction

The first observation of moving dislocations happened unexpectedly in a Siemens Elmiskop transmission electron microscope (TEM) operated at 100 kV in the Cavendish Laboratory of Cambridge University in 1956. The experiment has been related by Hirsch in more recent publications [1,2]. Dislocations started to move when the condenser aperture was removed and a sudden flux of electron caused the Al foil (thinned down by cold hammering and then annealed) to locally heat. This was sufficient to make a few dislocations move away from a sub grain boundary. In this first paper [3], many dislocation features were readily observable: dislocation emission from a sub-grain boundary, cross-slip between two planes, fabrication of temporary slip lines at the oxidized surfaces of Al served to prove that the moving defects were indeed dislocations.

This first report probably triggered the forthcoming hundreds of in situ TEM studies, with a common will to better control dislocation activity and possibly measure related parameters such as stress and strain.

One of the simplest mechanical tests consists in uniaxially pull on a sample of a given section while simultaneously measuring the load and the strain. This is currently done in large machines, available commercially. The sample has centimeter dimensions typically. Its change in length is measured through extensometers or optical cameras and is afterwards transformed in strain through the ratio to the initial gauge length. The applied force, measured through a load cell is converted to stress by dividing it by the gauge section. The resulting stress–strain curve (Fig. 1a) can be divided in the elastic (or reversible) regime where a suppression of the applied stress causes the sample to return to its initial state and a plastic (irreversible) regime where the same stress suppression leaves the sample deformed. In usual temperature and pressure conditions, the transition between both regimes (point 3, often called yield stress or (σ_y) coincides with the first irreversible motion of a dislocation, although such atomic-scale event is practically undetectable in macroscopic samples and is arbitrarily taken at 0.2% of plastic deformation (point 5 in Fig. 1a).

The most straightforward idea to reproduce a mechanical test in a TEM was to build a tensile machine that would fit inside the column, setting challenges that microscopists still face today. The dimensions of the straining unit and the associated sample (Fig. 1b–d) have to be drastically reduced. One can foresee the first challenge associated with this shape that includes an electron-transparent zone in the middle: the gauge section is poorly defined, and as a consequence, classical stress measurement will inherit such uncertainty. Because the high voltage TEMs ($\geqslant$1 MeV) that were developed in the 1960s and 1970s offered a pole piece gap of about 10 mm or larger, several research groups took advantage of this increased space to build custom-made straining stages, both for top entry and side entry microscopes. Some of these holders were remarkable mechanical testing units, capable to measure load, strain, and to operate from cold to hot temperatures [4,5]. Fig. 2 shows such a unit with the corresponding stress–displacement curves for pure iron deformed at various temperatures [5].

Another advantage of high voltage machines was their ability to see through large thicknesses of material (several microns of Al for example). This ability was judged important to avoid thin foil artifacts (see below) that have been a long-term concern for metallurgists. It also allows seeing how 3D dislocation structures establish and how dislocations interact with other structural defects. Since these linear defects have long-range elastic fields, typically of the order of one micrometer, thicker samples were capable to better reproduce interactions as they happen in the bulk material. Investigations on the potential thicknesses attainable with high energy electrons was even practically tested by building an ion milling system inside such HVEM (3.5 MeV in Toulouse, [6]). Of course, one of the drawbacks of these high voltage machines when it came to investigate the mechanical properties of metals and their relation to microstructures was that the irradiation threshold is often exceeded.

Nonetheless, the amount of work performed at that time, and their insight in the understanding in the dynamic evolution of defects under stress is worth to be remembered. Several workshops were organized, essentially between Japan and Europe, in Oxford, Kyoto, Holzau, Nagoya and Toulouse with available proceedings [7–11]. One can notice through these publications the transition from HVEM to regular 200–300 keV TEMS for in situ testing. A more recent paper published by Louchet and Saka that were part of this scientific adventure, may be seen as a good starting review [12]. To have a comprehensive view of the in situ TEM activities up to 2010, readers are kindly but firmly invited to refer to the excellent book about the dynamics of dislocations in various materials by Messerchmidt [13].

Various approaches of mechanical testing inside a TEM exist today. They span from using TEM holders with a simple mechanical actuation (Section 2.1) or rely on elaborated testing units that fit inside the pole pieces (Section 2.3). With the miniaturization of MEMS (Micro Electro Mechanical Systems), one can also fabricate such a testing machine on a few mm^2 of Si, and plug it inside the TEM through simple electrical connecting holders (Section 2.3.3). Finally, straining materials can also be achieved by playing with various coefficients of thermal expansion (Section 3).

Moving dislocations, considered as elastic probes, allow the access to quantities such as local shear stress, activation energies, and obviously strain that can be analyzed to access fundamental parameters of the plastic properties of the material at a given temperature, stress and time (Section 4.1). Finally, TEM imaging also contains some information that can be retrieved to access mechanical variations (Section 4.2 Coupling factor, strain and stress field, CBED, holography).

E-mail address: marc.legros@cemes.fr.

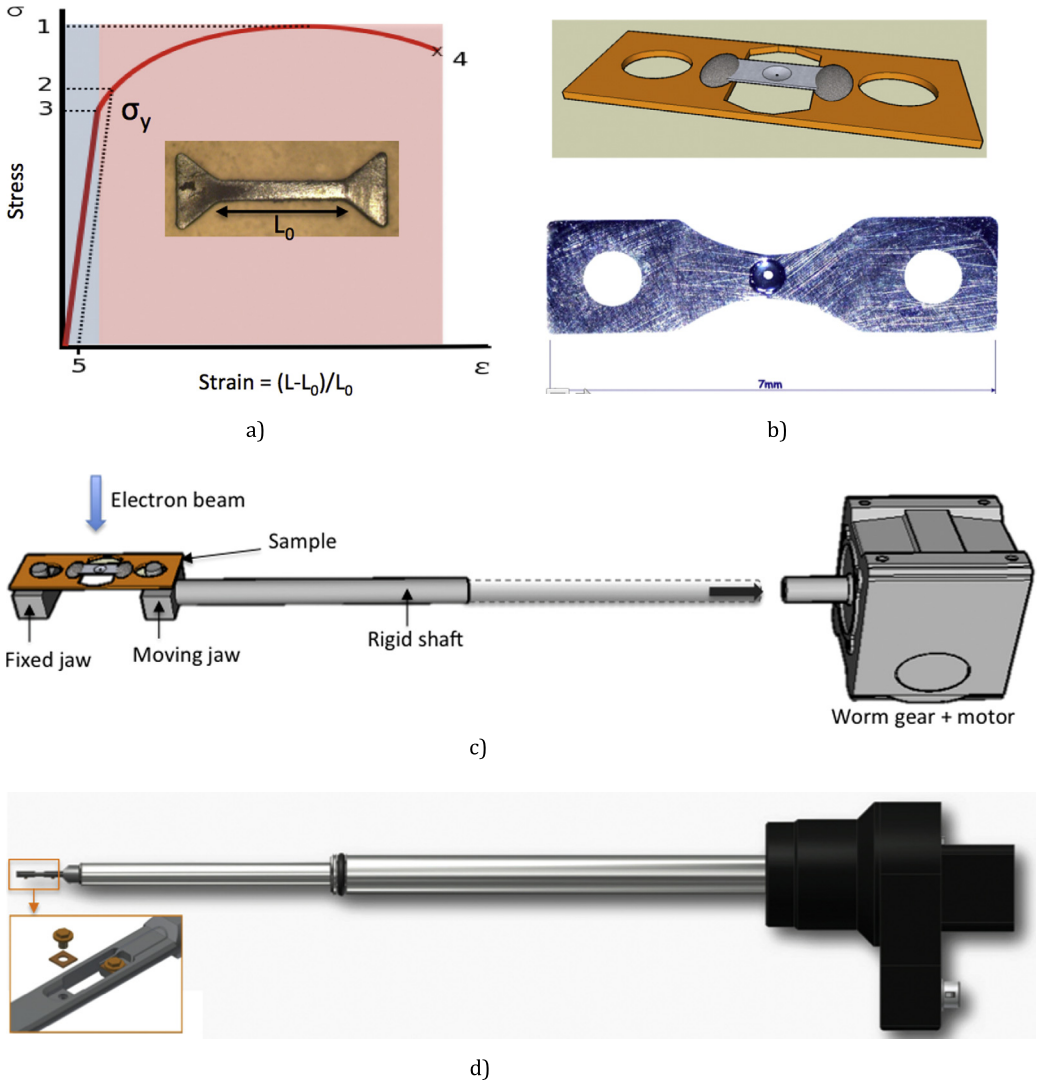

Fig. 1. (Color online.) a) Schematic stress–strain curve for a uniaxial tensile test performed on a macroscopic dog-bone shaped specimen (insert). Point 3 corresponds to the transition between elastic (gray) and plastic (pink) regimes of the curve. The corresponding stress is called the yield stress or σ_y. b) Samples for *in situ* TEM straining. Rectangular shaped sample glued on a copper grid (upper right) or directly shaped as a dog bone (lower right). Note the dimple at the center of both samples, where e-transparency is achieved. c–d) Standard straining holders based on electric motor and worm gear actuation. c) Principle, d) commercial room temperature holder for FEI microscope made by Gatan ©.

2. Mechanical straining holders

2.1. Classical tensile holders

With the almost standardized side entry stages, and reduction of voltage in modern microscopes, the basic straining holders are now available commercially. Their principle is described in Fig. 1c: the electron transparent sample is cut to shape or glued to a deformable grid (Fig. 1) that is compatible with the holder fixation system (pin, screw, clamp). This sample is stretched from a long rigid shaft attached to a worm gear box actuated by an electric motor and located in a housing outside the TEM. This allows straining speeds ranging from 10 nm/s to 10 µm/s, typically, although a given system rarely allows more than 2 decades in speed.

This simple set-up presents many advantages that make this type of holder widely used today:

- Extreme **versatility**. Any thin or thinned sample can be strained as soon as it is transported and glued to a stretchable grid [14]. Nowadays, objects as small as nanowires or thin films can be transferred and glued with the help of micromanipulators.

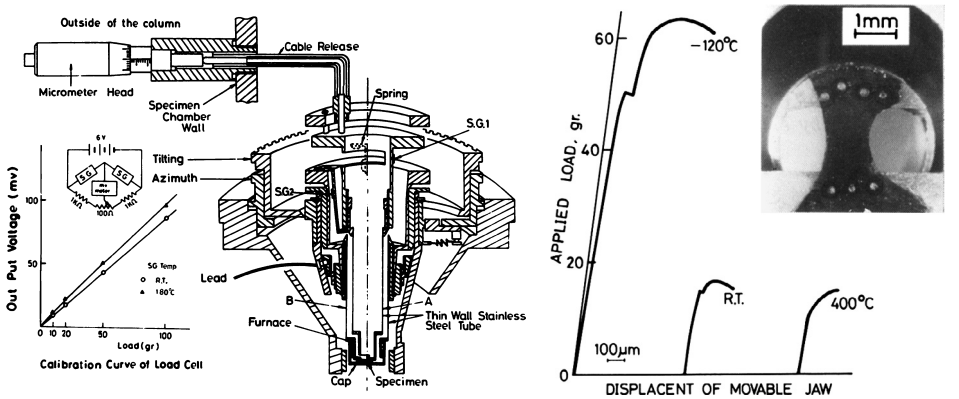

Fig. 2. Early developments in HVEM in situ straining stages. a) Top entry manual straining holder custom fabricated for the HVEM in Nagoya (1973), b) stress–strain curves obtained at various temperatures inside the TEM. Insert shows the Fe sample welded at both upper and lower ends of the straining tube [4].

- **Heating or cooling** options. They are commonly added to this type of holders. Cooling is usually monitored from outside through a cold finger itself connected to a liquid He or N2 reservoir. Heating is performed through a miniaturized furnace that can typically reach 1000 °C or through laser for higher temperatures [15].
- **Rigidity**. The reduction in sample dimensions to create an electron transparent zone favors crack propagation and increases the probability of brittle failure. The very rigid displacement transmission allows to deform thin films [16,17] or brittle alloys [18]. Incorporating a load cell [19] or a double tilt capability [20] implies to soften the transmission of the strain and can therefore be detrimental in controlling crack propagation.

The classical in situ straining technique, including sample preparation and mounting, stress concentrations, possible artifacts have been discussed in [21]. Other custom-made holders expanding from a simple straining actuation can be found in the literature such as a double tilt straining holder [20], bending holder [22] and pure shear holder [23,24].

2.2. Nanoindentation holders

Nanoindentation, or instrumented indentation is a technique that appeared in the early 1980s and consists in measuring the force and displacement of a hard tip forced into a material, previously polished flat. This technique allows retrieving the hardness but also the elastic modulus of the tested material, and in certain conditions, the yield stress [25]. The force and displacement are usually measured through a change in capacitance between a reference and a movable electrostatic plate attached to the tip [26–28].

In the 1990s, several holders were developed taking advantage of the very accurate positioning capabilities of piezoelectric stacks and tubes to bend, pull or compress samples as small as carbon nanotubes [29–33]. Rapidly, nanoindentation tips were attached on top of these piezo-actuated holders to locally deform metals [34–36]. The results obtained in term of plasticity mechanisms had a strong impact but were also criticized [37,38]. From 2003 to 2005, two companies further implemented these indenting holders by adjoining them a micro load cell. Hysitron® [39] constructed a TEM nanoindenter with a loading mode based on the capacitance variation similar to the one in large scale nanoindenters [40,41]. This piece of equipment was only available for JEOL microscope before being adapted to other TEMs. Nanofactory Instruments AB® chose to take advantage of the compactness of Micro Electro Mechanical Systems (MEMS, see Section 2.3) [42,43] to propose nanomechanical testing units that could fit more TEMs and different force ranges. AFM holders were also proposed. In England, Inkson and coworkers also developed a custom piezo-actuated nanoindentation holder, but in that case, the load was not read electronically, and one had to measure the displacement of a calibrated spring platform [44], similar to what is proposed in some passive MEMS system (see Section 2.3.1).

Beside their load sensors, Nanofactory and Hysitron holders differ in several ways: The Hysitron construction resembles a classical indenter set up where a hard tip is pressed against a sample that is fixed. Mechanical micrometers located on the back of the holder enable the coarse positioning of the sample with regards to the electron transparent window. Fine positioning is provided by a piezo tube in the three dimensions x, y, z (z being the electron beam direction and x the indentation axis, see Fig. 3a). In the Nanofactory holder [45], the tip is fixed on the top of the force sensor that is immobile. The coarse and fine motion of the sample towards the tip are both carried out by a four-leg gripper attached to a conductive ball itself soldered on a piezoelectric tube. Coarse motion is achieved through stick–slip motion while fine displacements are controlled by the continuous motion of the piezo tube. Maximum loads accessible with such instruments are typically lower than 10 mN, while the floor noise sets below a μN. Smaller load cells were accessible at Nanofactory Instruments AB

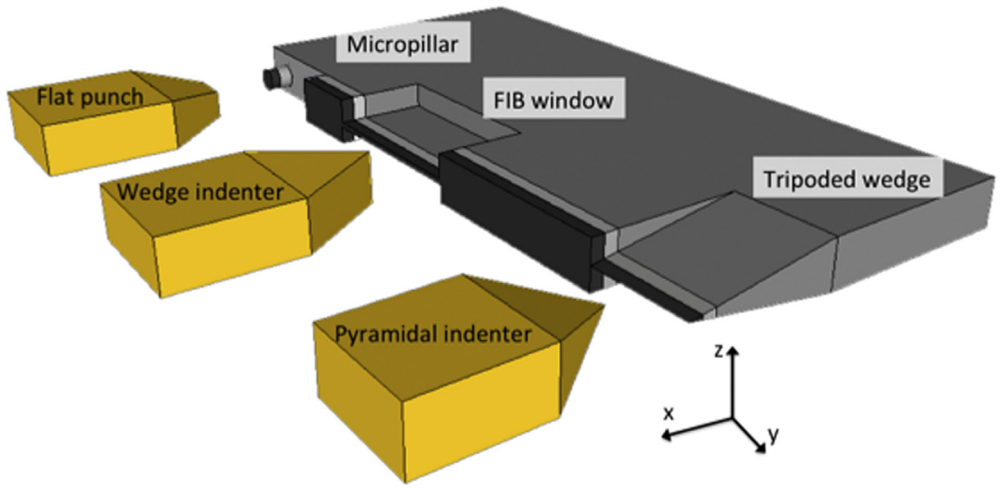

a)

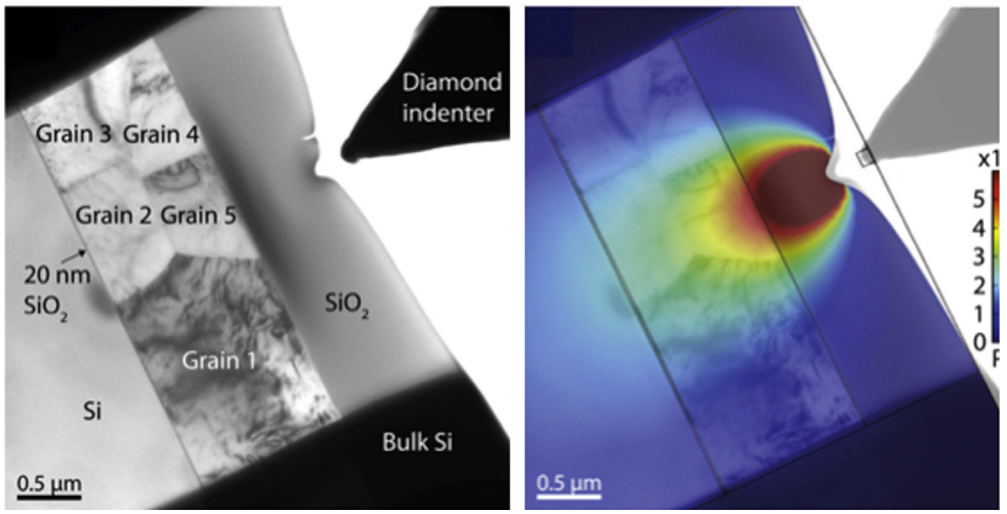

b) c)

Fig. 3. (Color online.) Indentation holder configurations. a) Sample can be prepared as a H-bar window or a micro-nanopillar using FIB, or as a wedge with a tripod polisher. Tips can be either pyramidal (sharp tip), wedge-shaped elongated in the z direction (along the electron beam) or flat punch-type. a–b) A FIB-made window in situ indented inside a TEM. b) Bright field TEM image, c) Superimposed FEM Von Mises stress field during indentation on image b) (from [50]).

before the company ceased activity in the beginning of 2013 [46] and was bought by FEI. At the time this paper is written, it is not clear what will be the future of Nanofactory holders manufacturing.

In order to be indented, the TEM sample has to offer a free half space ($x > 0$ in Fig. 3a) to let the tip access the desired location, and at the same time, this location has to be transparent to electrons. The first sample investigated was an Al layer deposited on a Si wedge [47], but more standard samples are nowadays shaped as wedges or H-bars as in Fig. 3a. As one can anticipate from Fig. 3a, a primary difficulty with nanoindenting holders is to set both the tip and the sample at the same height in the eucentric location of the TEM. The precision, in the case of the pyramidal (or conical tip) is of the order of 10 nm. The introduction of wedge indenters with a length along z of about 1 to 3 microns typically, greatly facilitates the contact and prevents slipping while indentation is performed.

The second intrinsic drawback of such mechanical test is that, as the configurations of Fig. 3 underline it, this is neither a compression test nor a real indentation test where know approximations can apply [48] since both the tip and the sample geometries are complex and none of them is a flat surface, obviously. It is therefore almost necessary to perform Finite Element Mappings to quantitatively determine the stress transmitted to the sample (Fig. 3b, c). The contact of the tip with the sample creates a very strong gradient of deformation, which also precludes maintaining good imaging conditions during the deformation. This can be partly overcome only by capturing dynamic sequences in dark field [49] or by correcting the

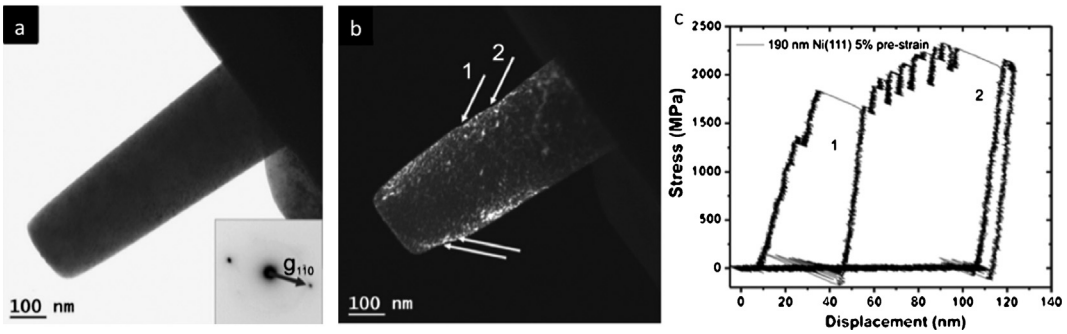

Fig. 4. Ni Micropillars compressed in situ using a flat-punch diamond tip mounted on a nanoindentation holder (after [68]) a) Bright field image prior to compression, b) Dark field imaging after compression, c) Stress–displacement curve calculated from the load measured by the nanoindenter.

bending as the tests goes on. In this Ref. [50], FEM calculations were matched with curvature radii of moving dislocations (see Section 4.1).

Flat punches tips can also serve to compress nanoparticles, but there too, modeling of the deformed sample is needed to really obtain quantitative data [51,52].

Working with samples that have a constant section allows to better taking advantage of the load measurement capabilities of these nanoindentation holders. A main target of such holders seems to be the deformation of nanopillars [49,53], which is an *in situ* TEM replication of micropillars compression testing that appeared in the classic experiment of 2004 by Uchic and co-workers [54]. Because of the intriguing size effect observed on strength, these pillar experiments opened an entire micromechanical testing domain [55–58]. For these micro-compression tests, the diamond sharp indenter is replaced by a flat punch.

However, the dimension range accessible for pillars in the TEM is more restricted than in the studies previously mentioned. They cannot be thicker than 100–300 nm depending on the material, and the FIB preparation induces many damages on the surfaces (one can see the typical white dots in the dark field image of Fig. 4). This also precludes the investigation of the strength of very small objects (<50 nm) that would be prepared by FIB. These implantation damages can strongly influence the mechanical response of the pillars [59], and other preparation routes have been preferred since then [60–62]. In situ experiments seem particularly suited to test dislocation exhaustion theories that are supposed to rule the mechanical properties of small single crystals [63]. Although mechanical annealing [53] seems much less effective than classical annealing [64], the change in contrast in compression is a major obstacle to clearly see dislocation and therefore assess for their density. Dislocation densities were better measured in tension [61,65], and do not show exhaustion nor starvation, only a decrease of initial FIB-induced defects [66] or a non-critical escape of dislocations near surfaces [67].

The use of nanoindentation holders in tension was first proved possible by using negative shape grippers, directly carved in the diamond tip [66,69]. This technique is however extremely time consuming and requires long milling times or specific lithography techniques [70].

A more general way of transforming a compression force into tension is to use so-called “Push-to-pull” (PtP) devices, often made in Si through lithography techniques. They are described below.

2.3. Micro Electro Mechanical Systems (MEMS)

2.3.1. Passive MEMS

Push-to-pull (or “PtP”) devices are among the simplest MEMS to build as they can be processed in very few lithography steps. Made out of Si wafers, they consist in a platform on which a pushing force is applied (usually using nanoindentation holders), and a pair of facing pads on which the sample to be pulled is attached, often using GIS (Gas Injection System) metal deposition in FIB microscopes. A geometry with arms producing antagonist movements connects the indentation site and the tensile pads. The Θ (Theta) shape is a popular one, as in the example of Fig. 5, engineered by Lou and co-workers [71,72]. In this set-up, the sample is located in the middle of the MEMS and a compression on the outside of the structure provides tension in the central gap (Fig. 5b). The resulting stress–strain curve has to be corrected by removing the stiffness of the empty PtP. This can be done once the sample is broken, or before the mounting of the specimen. Of course, the dimensions and subsequent stiffness of the PtP has to be adapted to the load range investigated, and, compared to micron-sized fibers, nanowires (diameter lower than 50 nm) needs much smaller devices.

2.3.2. Co-fabrication (testing platform and sample)

To avoid micromanipulation (harvesting, welding) of micro- and nano-samples (wires, fiber, films), the co-fabrication of the sample with its testing frame is also possible. A U-spring-shaped Si structure supporting a nanocrystalline Al film processed using vapor deposition has recently been fabricated and tested successfully using a simple straining holder [16]. In this case, the MEMS design facilitates the handling of the film (otherwise difficult [75]) and helps preventing early fracture of the nanocrystalline film by opposing an elastic force around the sample.

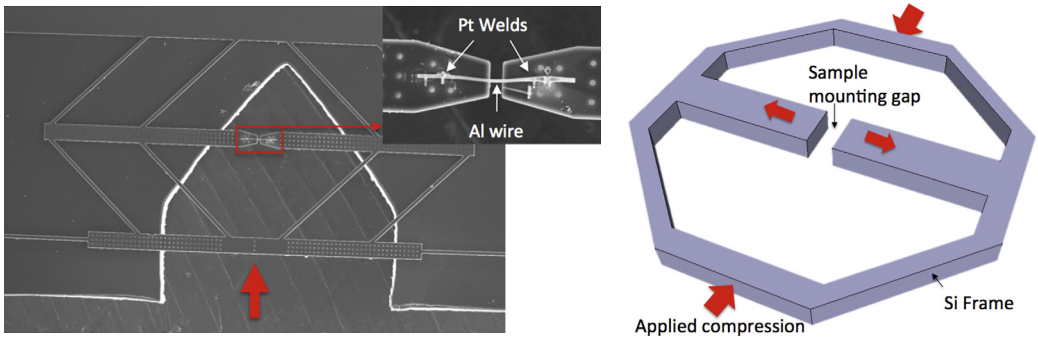

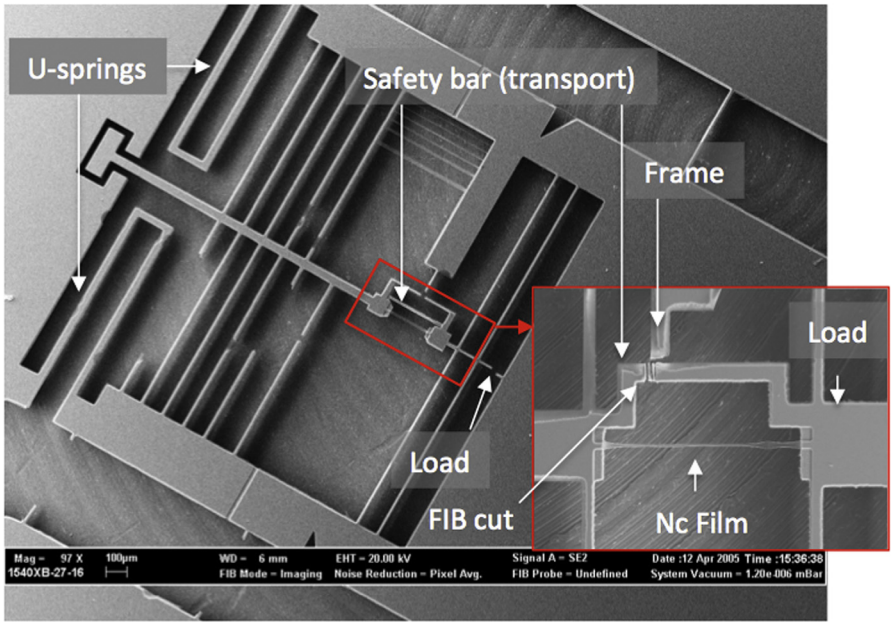

Fig. 5. (Color online.) Passive MEMS structures for mechanical in situ TEM testing. a–b) Push to Pull device fabricated through Si lithography and mounted sample using Pt deposition (insert) (PtP provided by J. Lou [71]), the length of the red box (insert) is 100 µm, b) mechanical principle to transform a compression force into tension (Theta shape), c) Tensile MEMS structure including a co-fabricated nanocrystalline (nc) film, allowing for stress–strain measurements using Si beams deflections. This sample can be loaded using a classical or piezo-driven tensile holder [73,74].

These tensile MEMS were inspired from much more complex passive structure designed by Saif and co-workers where deformation and load can be measured through the relative displacement of Si beams that have a known stiffness [76–78]. In such design (Fig. 5c), three markers located near the thin film serve to calculate the load and the strain. The load is derived from the deflection of Si beams that have known dimensions and thus known stiffness. The thicker these beams are, the larger the measured load can be and the lower the resolution is. The deformation is obtained by subtracting the displacements of Si beams at each end of the sample. Several designs have been created. In the one described in the insert (Fig. 5c), the three markers (Reference, Load, Safety) are created by FIB-cutting the T-shape Si Safety beam in three parts. In the larger picture, the three markers are fabricated using lithography, and a safety bar (to prevent early failure of the film during transportation) has to be FIB-cut before the test.

Although this set-up allowed some results on nanocrystalline samples [79–81], it carries some inconvenient:

- Some large-scale cuts (several μm^3) have to be made using FIB. This is potentially contaminant for the nearby nc films, especially if this one is Al-based, as Ga is a known source of embrittlement for Al grain boundaries.
- The measurements are slightly away from the film, which means that one has to constantly switch between the sample position and the markers position to follow the mechanism unraveling in the film and acquire measurements for stress and strain.
- The film is very long, which makes it difficult to locate the deforming zone, often very narrow.

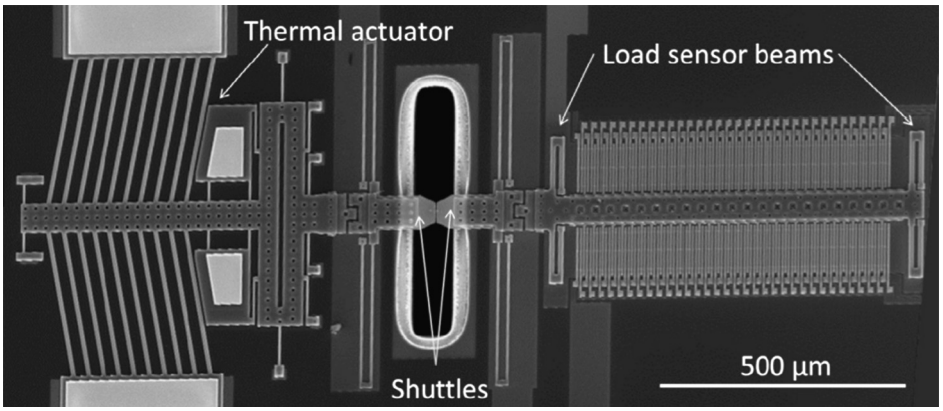

Fig. 6. Active MEMS stress–strain measurement platform for nanowires and carbon nanotubes, from [84].

- The stiffness of the machine is also limited, which implies that once the deformation starts in the sample, the elastic strain accumulated in the Si beams cannot insure a rigid deformation of the sample and may cause its rapid failure. The chances to observe a deformation process at a low strain rate, compatible with current CCD camera rate, become scarce.

2.3.3. Active MEMS

In order to avoid some of the drawbacks mentioned above, some MEMS devices have been designed with built-in actuators and sensors. Injected electrical power serves to apply a stress, while capacitance variations can be calibrated to directly return a displacement or strain. Espinosa and co-workers were among the first to develop such platforms [82,83].

In the example of Fig. 6, the V-shaped Si beams (on the left) expand when traversed by an injected current, imposing a uniaxial tensile displacement to the shuttles on which samples are to be mounted (W or Pt weld such as in Fig. 5). The Si combs on the right are capacitances that, once calibrated are precise displacement sensors. They are attached to Si beams with known stiffness that serve as load sensors. Typical loads are in the range of µN, while displacement remains very limited, rarely above a couple micrometers.

In this set-up, the strain (deformation of the sample relative to its initial length) has to be calculated after the test and may be influenced by the relative rigidity or softness of the sample. The amount of heat injected in the actuator may also be conducted to the sample, introducing a potentially unwanted temperature change that may significantly affect the results [85]. This is the reason why other teams have recently included thermal barriers (epoxy-glued pads) and double capacitance readouts at each end of the deforming sample [86].

Finally, very low forces (1–100-nN range) can be accessed through MEMS-based devices that are actuated electrostatically [87]. This is particularly useful to study nanojunctions or friction near the atomic level [88,89]. AFM-based TEM holders have also been developed by Nanofactory Instruments AB, with force resolutions of about 10 nN.

The bibliography on MEMS devices related to in situ TEM (not limited to mechanical testing) is becoming extremely vast. A recent review has been recently published that gives a substantial, although slightly skewed of the field [84].

3. Straining based on difference in thermal expansion

Stress and strain impact in microelectronics engineering can be negative (device failures [90]) or positive (strained Si [91]) and TEM investigations have significantly contributed to the field. After relating interfacial dislocation to misfit strain between two semiconductor layers [92–94], it is now possible to map the strain and stress field in a constrained Si channel using electron holography [95]. These techniques are however static, and equivalent dynamic observations are still to be made.

Regarding threading and interfacial dislocations, metal layers deposited on Si substrates have been considered as semiconductors [96,97], but due to the much easier generation and multiplication of dislocations and defects in metals, this comparison failed to truly capture the mechanical properties of metals on substrates.

Because they are often used as interconnects, electric power spread over electronic devices causes a global heating through Joule effect. With increased integration and downscaling, power concentrations and heat evacuation become an issue. Mechanically, heat cycles cause stresses that originate from the difference in coefficient of thermal expansion (CTE) between metals, oxides and semiconductor parts. The metal (often Au, Al, Cu, W ...) is the softer part, with the highest CTE, and therefore is prone to plastically deform. Usual macroscopic thermo-mechanical tests are run using a so-called wafer-curvature experiment: the stress induced in the expanding metal film by thermal cycles imposes a radius of curvature to the substrate. The relation between this radius and the stress is given by the Stoney formula [98,99]. For most metallic films studied by this method, a strong size effect was found: the thinner the film, the higher the stress needed to plastically deform it [100].

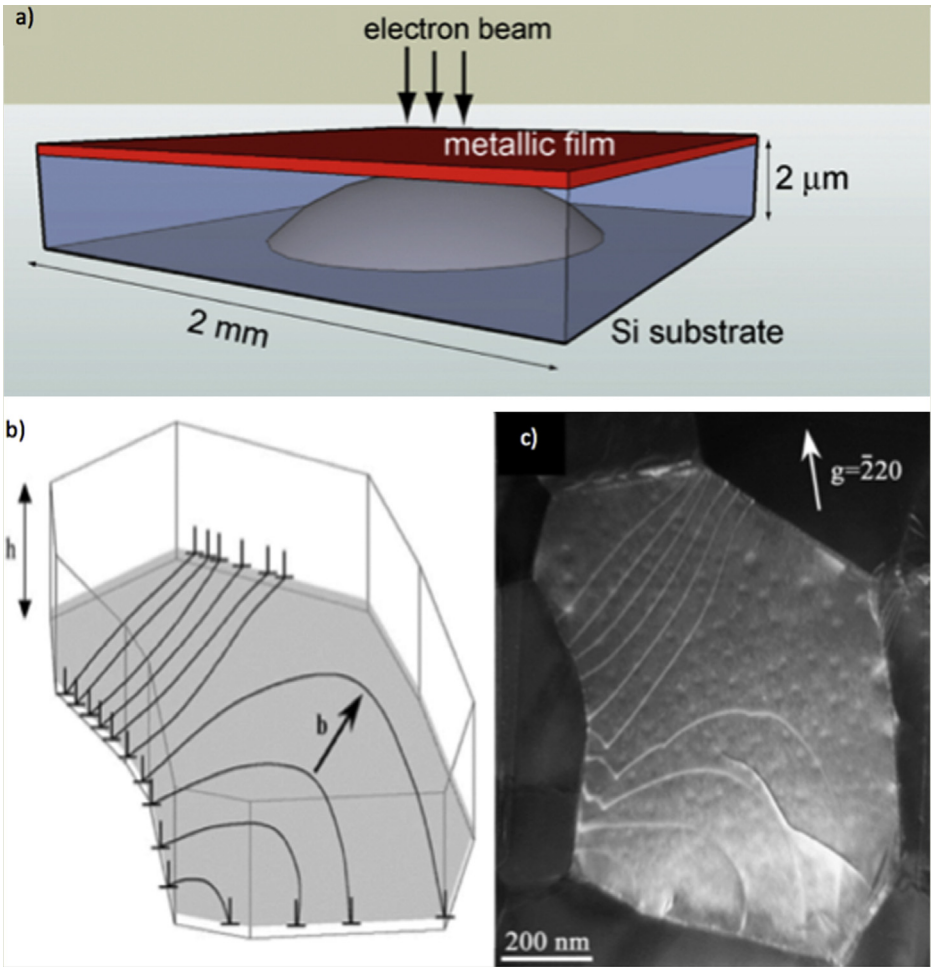

Fig. 7. (Color online.) Plane view straining of thin film on substrate based on the difference of CTE. Substrate is back-thinned to a few tens of nm and the metal film has to be e-transparent too (a). For thin ($h \leqslant 200$ nm) polycrystalline Cu films, dislocations parallel to the substrate expand from GB triple junctions (b, c). Their motion is almost fully reversible with temperature (picture (c) is taken at 40 °C during a cooling phase from 355 °C) [45].

Metallic films on substrate are supposed to deform through the propagation of threading dislocations, but their observation in metals have been controversial [101], especially in the case of oxidized substrates where an amorphous layer separates the silicon from the metal [50,102]. This topic is of theoretical importance because the image forces that rule the dislocation–interface interaction at the metal/substrate junction are supposed to cause the "thinner is stronger" size effect in thin films [97]. It has also practical implications since metal/oxide or metal/semiconductor interfaces are the base of material stacks in microelectronics.

In situ TEM presents again the very unique capability to observe this interaction, but the geometry of the specimen has to be adapted to keep the interface either in plane view or in cross-section [22]. Heating experiments on metal/Si substrates TEM specimen proved to be able to reproduce partly the stress levels experienced by metals in wafer curvature experiments [103–107]. As predicted by continuum elasticity, it has been shown that threading dislocations are repulsed from a stiff crystalline interface (sapphire [108,109]). Inversely, dislocations seem attracted by amorphous interfaces that act as a sink for small deformations in the metal [50,102]. This sink effect also prevents from stress concentration and further dislocation multiplication, which may explain why metals on oxide systems appear stronger during thermal cycles [106,110].

In fact in situ TEM revealed an even more surprising behavior. Observing very thin polycrystalline Cu films strained in plane view using the difference of CTE between the metal and the Si substrate (Fig. 7), Balk and co-workers observed the initiation of so-called "parallel dislocations" [111]. These dislocations are not activated by the applied stress (which component is nil on the interface), but seems to be the result of grain boundary diffusion, as predicted by a recent model for polycrystalline thin film relaxations [112,113]. By just counting the dislocations emitted and absorbed (the process is almost perfectly reversible) at the GB-interface junction, one can quantify this unusual relaxation mechanism. This pure in situ TEM discovery appears as the perfect complement of classical threading dislocation models for metals on oxidized substrates.

4. Measuring stress and strain from moving dislocations and TEM images

Electron–matter and especially electron–crystal interactions provide very rich images from which strain and stress can be sometimes extracted.

4.1. Moving dislocations

Dislocations are defects that are on one hand easily imaged by TEM, and also entirely ruled by the elastic properties of the crystal lattice they belong too. Their shape and mobility are direct indications of the local stress state. Each dislocation carries a strain quantum equal to its Burgers vector, providing the ultimate shear strain measurement in plasticity.

A dislocation loop in its glide plane subjected to a shear stress will bend, balancing the applied stress by its line tension. This is especially visible when the lattice friction is low, as in fcc metals (Au, Al, Cu…) at most temperatures. Curved dislocations also carry out the plastic deformation in the easy glide direction of hcp (Ti, Mg…) and bcc (Fe, Mo, W…) metals or when the crystal deforms at high temperature (above the critical temperature for bcc metals, close to melting temperature for semiconductors).

A simplified equation to link the shear stress acting on a dislocation to its radius of curvature R is [114,115]:

$$\tau = \frac{\mu b}{R}$$

where τ is the resolved shear stress (in the dislocation glide plane), **b** its Burgers vector, μ the shear modulus of the crystal.

This equation gives the local stress acting on a dislocation loop expanding inside a material at a given time. It also depends on its direct environment (other dislocations, interfaces, surfaces), which sometimes precludes a direct comparison with stresses measured on the corresponding bulk material. In small-size materials such as thin films, wires, pillars under stress, the local stress can be directly related to the relevant stress needed to reach plastically deformation. The resolved shear stress is related to the applied stress through the Schmid factor that links the angle between the glide plane and shear direction to the axis of the applied stress.

In Fig. 8, a spiral source was activated in an Al wire produced by selective etching of an eutectic alloy (to avoid FIB milling) [116]. This experiment was carried out in a simple straining holder, and repeated on fibers with different sections. The radius of curvature measurements showed that the “smaller is stronger” effect observed in these metal wires was directly related to the position of the source with respect to the surface: the closer it is, the smaller the critical radius of curvature has to be and the higher the stress needed to move the dislocation. In Fig. 8b, the bright-field TEM video capture taken at the onset of source activation was subtracted to the video capture taken after the emission of about 50 dislocations. The resulting shear (10 nm) measured on the left edge of the fiber is compatible with the projected shear produced by the mobile dislocations of the source (the Burgers vector is here directly determined as the common direction between the primary and cross-slip planes, see [116]). Of course, counting each dislocation exiting the crystal gives in real-time the most precise value of the shear strain seen by the wire (amplitude of the Burgers vector divided by the section). Real strain rates $\dot{\varepsilon}$ can be measured at the atomic scale through the Orowan equation:

$$\dot{\varepsilon} = \rho b v$$

where v is the dislocation velocity and ρ the density of mobile dislocations, both quantities that are only postulated at the macro scale. The stress measured from the radii of curvature was statistically compared with those measured using micro load cells in a SEM and the results were very similar, underlying the robustness of the in situ TEM measurements. In addition, mechanisms responsible for the deformation (spiral sources) were clearly identified [61]. This study exemplifies how in situ TEM may reveal the physical reasons of the strengthening or weakening mechanisms at work in small crystals.

The dislocation curvature method has been vastly used to measure in situ local shear stresses in pure metals [118,119], alloys [120–123], but the specific impact of thin foil testing (image forces, native oxide on surfaces) prevents from a direct transposition of local stresses measured inside the TEM to bulk samples strength. Additional strengthening mechanisms also need to be accounted for.

Lattice friction stress (or Peierls stress for semiconductors) is one of the known strengthening mechanisms that govern the plastic response of most of intermetallic alloys and bcc metals. In the TEM, this friction leads to the straightening of screw dislocations, much less mobile than edge segments [124]. Because of the sampling imposed by the volume of a thin foil, dipoles of straight screw segments form after the expansion of the initial dislocation loop and its curved non-screw (Fig. 8c). Their formation takes place as soon as their separation dc is such that the work done by the applied stress τ_a corresponds to the dipole energy, namely [115]:

$$d_c b \tau_a = \frac{\mu b^2}{2\pi} \ln \frac{d_c}{b}$$

where μ is the shear modulus and b the Burgers vector of the dislocations. A similar equation can be written for annihilating dipoles, and both observations can be considered as micro strain-rate variation tests, since the local interaction of dislocations will impact their velocity. Determination of real activation energies of the unfolding dislocations processes are reachable [117,124,125], which is again, a unique potentiality of in situ TEM mechanical testing.

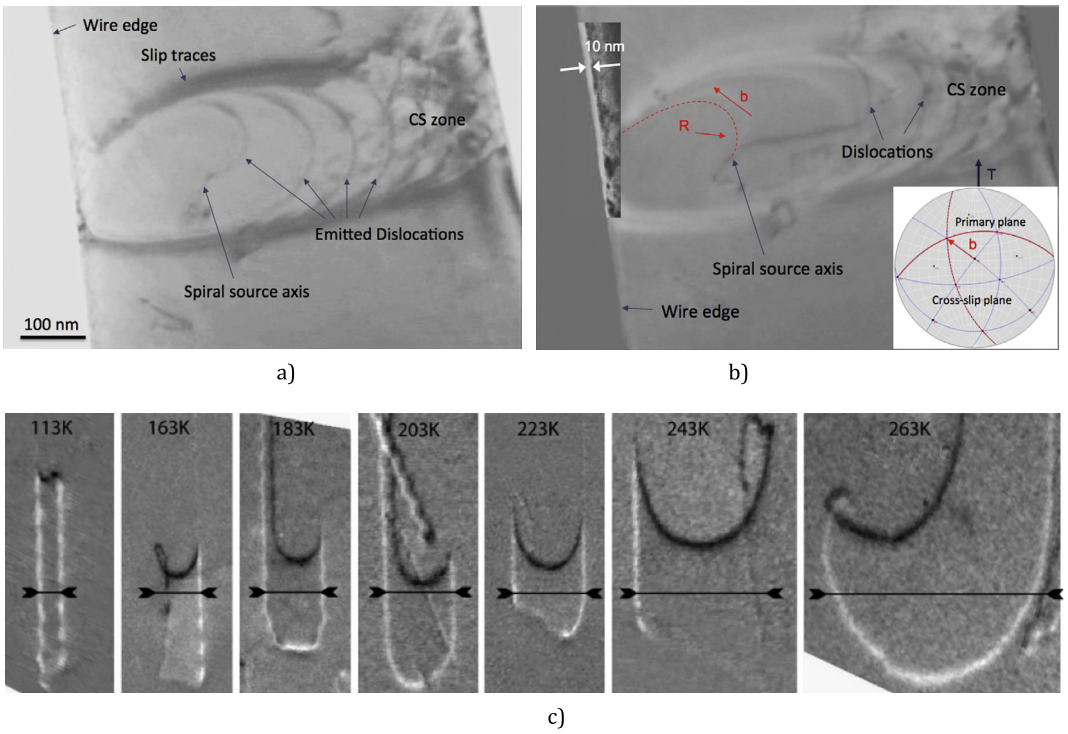

Fig. 8. Stress measured from mobile dislocations. a–b) Spiral source activated in a 700 nm wide Al wire deformed in traction. Radius of curvature measurements provide the local stress while the number of dislocation emitted accounts for the strain [61]. c) Dipoles expending in pure Fe at various temperatures. The arrows indicate the critical dipole width [117].

Knowing the applied and local stresses acting on dislocations opens other possibilities such as the determination of a microstructural obstacle strength, typically a precipitate, a grain boundary (GB) or a twin boundary (TB). These are known obstacles to dislocation motion, but they can be overcome by accumulating dislocations.

The stress at the tip of a pile-up is just the number of dislocations involved times the applied shear stress τ_a:

$$\tau = N\tau_a$$

where τ is the shear stress acting on the first dislocation in a pile-up containing N dislocations. This holds true even if segments of dislocations are piling up, as it is the case in thin foils [126].

This property has been recently used to estimate the stress needed to overcome a nanotwin in Cu, as illustrated in Fig. 9 [127], and to account for short-range order in Ni-based alloys [128].

4.2. Measuring strain in TEM images

As seen in Fig. 8, the subtraction of images captured before and after a shear event can reveal the amount of strain implied in dislocation processes. When the whole section is visible, the measurement is equivalent to what can be obtained at macroscopic scales. Image correlation is still done in a manual way since digital image correlation (DIC [129]) applied to TEM images is still poorly developed. The low resolution of video captures and the variation of contrast during an in situ test are still major obstacles to overcome before being able to perform DIC automatically [130–132].

Yet, this manual processing of images proved to be indispensable to capture at the nanometer scale a “new” plastic deformation process, namely shear-migration grain boundary (GB) coupling [133–138]. This mechanism, first revealed in low angle GBs, produces a shear mostly parallel to a GB moving along its normal. At variance from dislocations, the amount of shear produced by GB migration, the coupling factor, is not known a priori, despite recent articles tend to link this shear to the misorientation carried by the GB. This coupling factor β is defined by the amount of shear d divided by the migration distance m: $\beta = \frac{d}{m}$. It has been measured macroscopically for bi-crystals [139], but only recently at the nanometer scale and in the case of polycrystals [135,140]. The method employed consisted in straining ultra-fine grain (UFG: grain size $\leqslant$1 μm) Al samples between 350 and 400 °C and follow the relative displacement of gold nanoparticles dispersed on the TEM sample surface after some GB migrated (Fig. 10).

By comparing the displacement of markers that were not swept by GB motion (X1), to those who experienced migration (X2), it is possible to measure β. Here $\beta = 5\%$, which is a low value, typical of what is found in polycrystals [141].

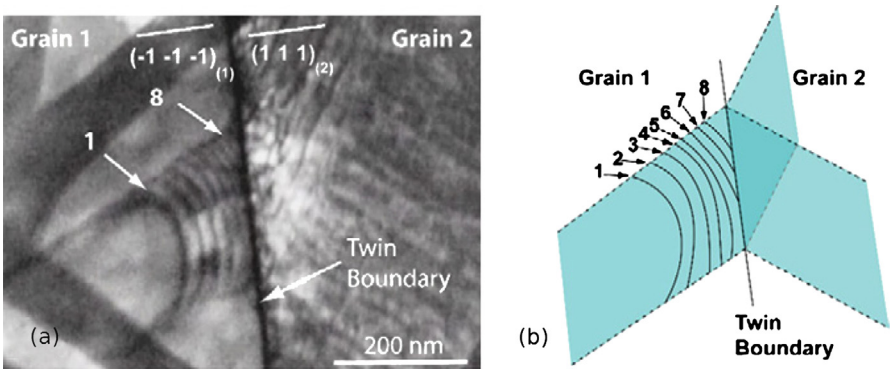

Fig. 9. Nanotwin boundary crossing at room temperature in Cu due to dislocations pile up at grain 1/grain 2 twin interface [127].

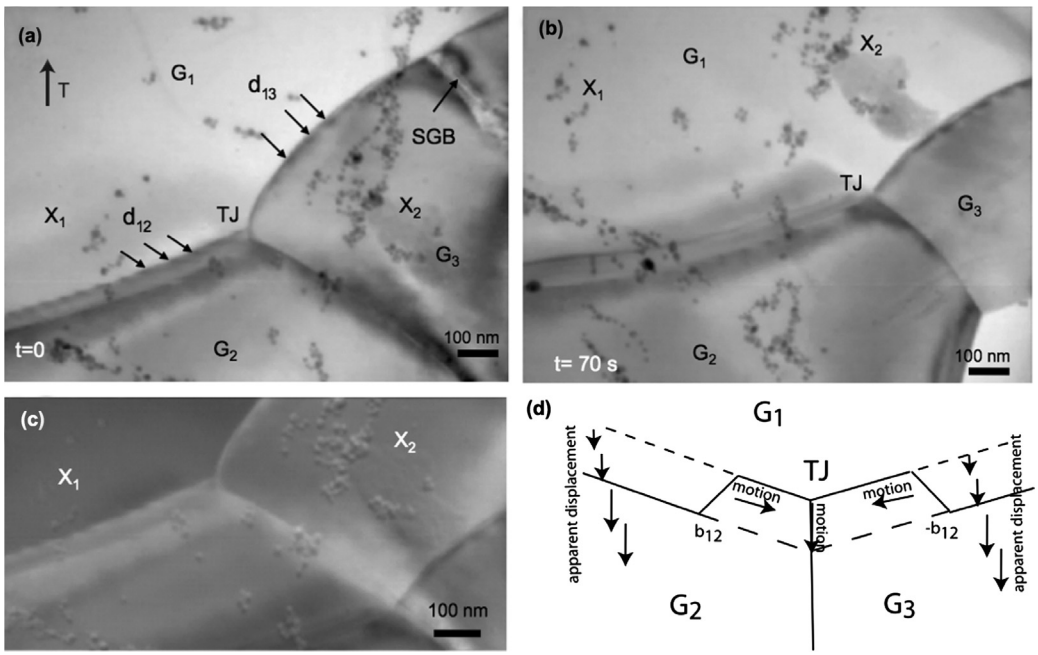

Fig. 10. Shear produced by GB migration around a triple junction (TJ) in UFG Al at 400 °C. The coupling factor β (see text) is here close to 5%. X_i are reference markers made of Au nanoparticles. a) and b) are image taken before and after the GB migration. c) is a subtraction of b) and a). d) shows how the migration occurs by step motion.

Several static TEM techniques can measure the strain in a sample in a much more precise way, either CBED (Convergent Beam Electron Diffraction) [142,143] or interferometry [95,144,145], but those techniques have not been applied successfully to in situ straining so far.

An attempt to use dark field holography to a Si sample was presented at the ICM17 [146] and is reproduced in Fig. 11. The set-up prior to indentation is shown in Fig. 11a after the tip and the sample have been set to the same level, which is a tedious process for all tip-type experiments. The initial hologram is shown in Fig. 11b and the corresponding normalized strain map obtained using the GPA plug-in [147] of Digital Micrograph © based on a reference zone of the crystal taken as far as possible from the indentation zone in Fig. 11c). During indentation, the strain map of Fig. 11d is obtained, showing a concentration of strain in the front tip of the sample, but some bending too, shown by lines of equal strains parallel to the edge.

The difficulty of such an experiment lies in various points:

- the faces of the sample have to be as parallel as possible to avoid thickness fringes that may interfere with the hologram;
- tilting is not possible during indentation as no goniometer motion is smooth enough today to avoid catastrophic mechanical vibration transmission to the sample;

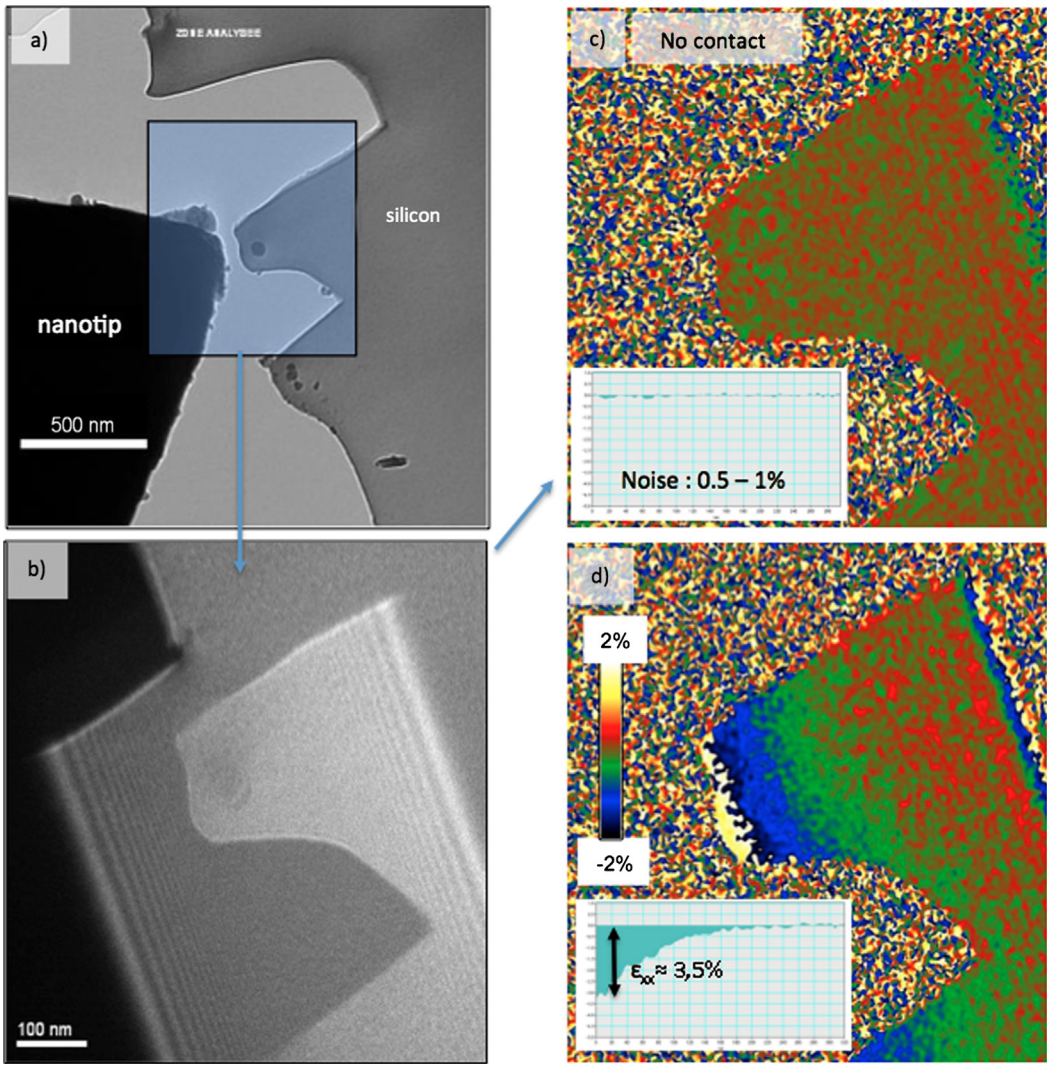

Fig. 11. (Color online.) Attempt to perform dark-field holography under in situ TEM nanoindentation. a) Diamond tip facing the Si sample. b) Hologram showing fringes in the Si prior to indentation. c) Normalized strain state prior to indentation (absolute noise is between 0.5 and 1%), d) strained state during indentation calculated along the indentation axis (compression), after [146].

- because of the never perfect alignment of the tip, or the slight geometrical defects of the sample/tip, bending is often occurring (as in the experiment of Fig. 11), which precludes an in plane analysis of strain;
- the tip may introduce interferences/reduce the field of view;
- a reference region not too far from the stressed one is needed to obtain absolute values from GPA analysis;
- a very sensitive and rapid CCD camera is needed to capture varying holograms with the lower noise possible.

Progress should therefore be done in the domain of holder and goniometer stability, but also in the resolution of fast cameras (CCD or direct electron detection cameras [148]), as well as in the preparation of samples. Obtaining thin TEM foils with perfectly parallel faces is still a difficult task, even with modern equipment such as low voltage dual beam FIB and focused Ar ion beam milling tools.

5. Conclusion

The complexity of equipment to perform in situ mechanical tests in a TEM has recently increased to allow more quantitative experiments: stress and strain can nowadays be measured from outside the microscope with miniaturized piezo actuators and load cells. MEMS-based experiments are rapidly growing as they offer a cheap and easily customizable platform to test a variety of very small samples (micropillars, nanowires, thin films).

However, the intrinsic information that can be retrieved from images themselves is still underexploited. Moving dislocations are the ultimate mechanical probes to achieve sub-nanometer strain resolution measurements. Their curvature and interactions with other defects can also return local stress measurements without interfering with observations.

The advent of image-based strain and stress measurement (such as dark field holography) has triggered the current quest to perform this technique in a dynamic fashion. Use of DIC-type measurements may also be possible, provided a constant contrast through the test and the eventual decoration of the TEM sample with markers. These achievements are nowadays possible, but require the combination of ultimate mechanical stability of the microscope, straining holder and goniometer supporting it. Fast and highly resolved cameras able to capture a dynamical in situ test are emerging, leading to new challenges in term of data analysis and storage.

Acknowledgements

The author would like to thank D. Caillard and F. Mompiou for their continuous will to improve in situ TEM at CEMES and their advice in writing this article. The European Projects ESTEEM1 and 2, as well as the MIMETIS project funded by the French Ministry of Research are acknowledged.

References

[1] P.B. Hirsch, Direct Observations of moving dislocations: Reflections on the 30th anniversary of the first recorded observations of moving dislocations by transmission electron microscopy, Mater. Sci. Eng. 84 (1986) 1–10.
[2] P.B. Hirsch, Direct Observations of moving dislocations: Reflections on the 30th anniversary of the first recorded observations of moving dislocations by transmission electron microscopy, in: B. Cantor, M.J. Goringe (Eds.), Topics in Electron Diffraction and Microscopy of Materials, Wiley, 1999, p. 1.
[3] P.B. Hirsch, R.W. Horne, M.J. Whelan LXVIII, Direct observations of the arrangement and motion of dislocations in aluminium, Philos. Mag. 1 (1956) 677–684.
[4] T. Imura, N. Yukawa, H. Saka, A. Nohara, K. Noda, I. Ishikawa, In-situ dynamic observation of dislocation motion at low and high temperatures by HVEM, in: P.R. Swann, C.J. Humphreys, M.J. Goringe (Eds.), The Proceedings of the Third International Conference on High Voltage Electron Microscopy, Academic Press, 1974, pp. 199–205.
[5] T. Takeuchi, Load-elongation curves of pure body-centred cubic metals at low temperatures, J. Phys. Soc. Jpn. 35 (1973) 1.
[6] G. Dupouy, Performance and applications of the Toulouse 3 million volt electron microscope, J. Microsc. 97 (2011) 3–27.
[7] P.R. Swann, C.J. Humphreys, M.J. Goringe, High voltage electron microscopy, in: Proceedings of the Third International Conference, Oxford, England, August 27–30, 1973, 1974.
[8] T. Imura, H. Hashimoto (Eds.), 5th International Conference on High Voltage Electron Microscopy, The Japanese Society for Electron Microscopy, 1977.
[9] U. Messerschmidt, F. Appel, J. Heydenreich, V. Schmidt, Electron microscopy in plasticity and fracture research of materials, 1990.
[10] F. Louchet, H. Saka (Eds.), French–Japanese Seminar on In Situ Electron Microscopy, November 9–12, 1992, Nagoya, Japan, Microscopy Microanalysis Microstructures, vol. 4, 1993.
[11] H. Saka, D. Caillard (Eds.), French/Japanese Workshop on In Situ Experiments, J. Microsc. 203 (1) (2001).
[12] F. Louchet, H. Saka, Comments on the paper: observation of dislocation dynamics in the electron microscope, by BW Lagow et al., Mater. Sci. Eng. A, Struct. Mater.: Prop. Microstruct. Process. 352 (2003) 71–75.
[13] U. Messerschmidt, Introduction, Dislocation Dynamics During Plastic Deformation, Springer Series in Materials Science, vol. 129, 2010.
[14] P. Castany, M. Legros, Preparation of H-bar cross-sectional specimen for in situ TEM straining experiments: A FIB-based method applied to a nitrided Ti-6Al-4V alloy, Mater. Sci. Eng. A, Struct. Mater.: Prop. Microstruct. Process. 528 (2011) 1367–1371.
[15] K. Bataineh, Development of precision TEM holder assemblies for use in extreme environments, University of Pittsburgh, Ph.D. dissertation, 2006.
[16] F. Mompiou, M. Legros, A. Boé, M. Coulombier, J.P. Raskin, T. Pardoen, Inter- and intragranular plasticity mechanisms in ultrafine-grained Al thin films: An in situ TEM study, Acta Mater. 61 (2013) 205–216.
[17] D.S. Gianola, S. Van Petegem, M. Legros, S. Brandstetter, H. Van Swygenhoven, K.J. Hemker, Stress-assisted discontinuous grain growth and its effect on the deformation behavior of nanocrystalline aluminum thin films, Acta Mater. 54 (2006) 2253–2263.
[18] G. Molenat, D. Caillard, Dislocation mechanisms in Ni3Al at room temperature. In situ straining experiments in TEM, Philos. Mag. A 4 (1991) 153–170.
[19] Web site: robertson.matse.illinois.edu, n.d.
[20] J. Pelissier, P. Debrenne, In situ experiments in the new transmission electron microscopes, Microsc. Microanal. Microstruct. 4 (2–3) (1993) 111–117.
[21] A. Couret, J. Crestou, S. Farenc, G. Molenat, N. Clément, A. Coujou, et al., In situ deformation in T.E.M.: recent developments, Microsc. Microanal. Microstruct. 4 (1993) 153–170.
[22] M. Legros, M. Cabié, D.S. Gianola, In situ deformation of thin films on substrates, Microsc. Res. Tech. 72 (2009) 270–283.
[23] L.P. Kubin, J. Lepinoux, J. Rabier, P. Veyssière, A. Fourdeux, In situ plastic deformation of metals and alloys in the 200 kV electron microscope, in: Proceedings of the 6th International Conference on the Strength of Metals and Alloys, 1982, p. 953.
[24] J. Lepinoux, L.P. Kubin, In situ TEM observations of the cyclic dislocation behaviour in persistent slip bands of copper single crystals, Philos. Mag. A 51 (1985) 675–696.
[25] T.Y. Tsui, W.C. Oliver, G.M. Pharr, Influences of stress on the measurement of mechanical properties using nanoindentation: Part I. Experimental studies in an aluminum alloy, J. Mater. Res. 11 (2011) 752–759.
[26] W.C. Oliver, J.B. Pethica, Patent US4848141 – Method for continuous determination of the elastic stiffness of contact, Google Patents, Google.com.
[27] J.B. Pethicai, R. Hutchings, W.C. Oliver, Hardness measurement at penetration depths as small as 20 nm, Philos. Mag. A 48 (1983) 593–606.
[28] J.-L. Loubet, J.-M. Georges, O. Marchesini, G. Meille, Vickers indentation curves of magnesium oxide (MgO), J. Lubr. Technol. 106 (1984) 43–48.
[29] H. Ohnishi, Y. Kondo, K. Takayanagi, Nature 395 (1998) 780–783.
[30] T. Kizuka, Atomistic visualization of deformation in gold, Phys. Rev. B 57 (1998) 11158–11163.
[31] T. Kizuka, K. Yamada, N. Tanaka, Time-resolved high-resolution electron microscopy of solid state direct bonding of gold and zinc oxide nanocrystallites at ambient temperature, Appl. Phys. Lett. 70 (1997) 964–966.
[32] P. Poncharal, Z.L. Wang, D. Ugarte, W.A. de Heer, Electrostatic deflections and electromechanical resonances of carbon nanotubes, Science 283 (1999) 1513–1516.
[33] Z.L. Wang, P. Poncharal, W.A. de Heer, Measuring physical and mechanical properties of individual carbon nanotubes by in situ TEM, Journal of Physics and Chemistry of Solids. 61 (7) (2000) 1025–1030.
[34] E.A. Stach, T. Freeman, A.M. Minor, D.K. Owen, J. Cumings, M.A. Wall, et al., Development of a nanoindenter for In situ Transmission Electron Microscopy, Microscopy and Microanalysis. 7 (6) (2001) 507–517.

[35] M. Jin, A.M. Minor, E.A. Stach, J.J.W. Morris, Direct observation of deformation-induced grain growth during the nanoindentation of ultrafine-grained Al at room temperature, Acta Mater. 52 (2004) 5381–5387.
[36] A.J. Lockwood, B.J. Inkson, In situTEM nanoindentation and deformation of Si-nanoparticle clusters, J. Phys. D, Appl. Phys. 42 (2008) 035410.
[37] Z. Shan, E.A. Stach, J.M.K. Wiezorek, J.A. Knapp, D.M. Follstaedt, S.X. Mao, Grain boundary–mediated plasticity in nanocrystalline nickel, Science 305 (2004) 654–657.
[38] M. Chen, X. Yan, Comment on "Grain boundary-mediated plasticity in nanocrystalline nickel", Science 308 (2005) 356c.
[39] Web site: hysitron.com.
[40] O.L. Warren, Z.W. Shan, S.A.S. Asif, E.A. Stach, J.W. Morris, A.M. Minor, In situ nanoindentation in the TEM, Mater. Today 10 (2007) 59–60.
[41] A.M. Minor, S.A.S. Asif, Z.W. Shan, E.A. Stach, E. Cyrankowski, T.J. Wyrobek, et al., A new view of the onset of plasticity during the nanoindentation of aluminium, Nat. Mater. 5 (2006) 697–702.
[42] K. Svensson, Y. Jompol, H. Olin, E. Olsson, Compact design of a transmission electron microscope-scanning tunneling microscope holder with three-dimensional coarse motion, Rev. Sci. Instrum. 74 (2003) 4945–4947.
[43] A. Nafari, A. Danilov, H. Rödjegård, P. Enoksson, H. Olin, A micromachined nanoindentation force sensor, in: Eurosensors XVIII 2004 the 18th European Conference on Solid-State Transducers, 2005, pp. 44–49, 123–124.
[44] M.S. Bobji, C.S. Ramanujan, J.B. Pethica, B.J. Inkson, A miniaturized TEM nanoindenter for studying material deformation in situ, Meas. Sci. Technol. 17 (2006) 1324–1329.
[45] Web site, Nanofactory User Group, Nanofactory-User-Group.org.
[46] Web site: News 8, Pmvz-Esteem.Cemes.Fr.
[47] A.M. Minor, J.W. Morris, E.A. Stach, Quantitative in situ nanoindentation in an electron microscope, Appl. Phys. Lett. 79 (2001) 1625–1627.
[48] W.C. Oliver, G.M. Pharr, An improved technique for determining hardness and elastic modulus using load and displacement sensing indentation experiments, J. Mater. Res. 7 (1992) 1564–1583.
[49] D. Kiener, A.M. Minor, Source-controlled yield and hardening of Cu (100) studied by in situ transmission electron microscopy, Acta Mater. 59 (2011) 1328–1337.
[50] L. de Knoop, M. Legros, Absorption of crystal/amorphous interfacial dislocations during in situ TEM nanoindentation of an Al thin film on Si, Scr. Mater. 74 (2014) 44–47.
[51] E. Calvié, L. Joly-Pottuz, C. Esnouf, P. Clément, V. Garnier, J. Chevalier, et al., Real time TEM observation of alumina ceramic nano-particles during compression, J. Eur. Ceram. Soc. 32 (2012) 2067–2071.
[52] J. Deneen, W.M. Mook, A. Minor, W.W. Gerberich, C. Barry Carter, In situ deformation of silicon nanospheres, J. Mater. Sci. 41 (2006) 4477–4483.
[53] Z.W. Shan, R.K. Mishra, S.A.S. Asif, O.L. Warren, A.M. Minor, Mechanical annealing and source-limited deformation in submicrometre-diameter Ni crystals, Nat. Mater. 7 (2008) 115–119.
[54] M.D. Uchic, D.M. Dimiduk, J.N. Florando, W.D. Nix, Sample dimensions influence strength and crystal plasticity, Science 305 (2004) 986–989.
[55] J.R. Greer, J.T.M. De Hosson, Plasticity in small-sized metallic systems: Intrinsic versus extrinsic size effect, Prog. Mater. Sci. 56 (2011) 654–724.
[56] C.A. Volkert, A.M. Minor, Focused ion beam microscopy and micromachining, Mater. Res. Soc. Bull. 32 (2007) 389–395.
[57] M.D. Uchic, P.A. Shade, D.M. Dimiduk, Micro-compression testing of fcc metals: A selected overview of experiments and simulations, JOM 61 (2009) 36–41.
[58] M.D. Uchic, P.A. Shade, D.M. Dimiduk, Plasticity of micrometer-scale single crystals in compression, Annu. Rev. Mater. Res. 39 (2009) 361–386.
[59] H. Bei, S. Shim, M.K. Miller, G.M. Pharr, E.P. George, Effects of focused ion beam milling on the nanomechanical behavior of a molybdenum-alloy single crystal, Appl. Phys. Lett. 91 (2007) 111915.
[60] A.T. Jennings, M.J. Burek, J.R. Greer, Microstructure versus size: mechanical properties of electroplated single crystalline CU nanopillars, Phys. Rev. Lett. 104 (2010) 135503-1-4.
[61] F. Mompiou, M. Legros, A. Sedlmayr, D.S. Gianola, D. Caillard, O. Kraft, Source-based strengthening of sub-micrometer Al fibers, Acta Mater. 60 (2012) 977–983.
[62] P.S. Phani, K.E. Johanns, G. Duscher, A. Gali, E.P. George, G.M. Pharr, Scanning transmission electron microscope observations of defects in as-grown and pre-strained Mo alloy fibers, Acta Mater. 59 (2011) 2172–2179.
[63] J.R. Greer, W.D. Nix, Nanoscale gold pillars strengthened through dislocation starvation, Phys. Rev. B 73 (2006) 245410.
[64] M.B. Lowry, D. Kiener, M.M. LeBlanc, C. Chisholm, J.N. Florando, J.J.W. Morris, et al., Achieving the ideal strength in annealed molybdenum nanopillars, Acta Mater. 58 (2010) 5160–5167.
[65] S.H. Oh, M. Legros, D. Kiener, G. Dehm, In situ observation of dislocation nucleation and escape in a submicrometre aluminium single crystal, Nat. Mater. 8 (2009) 95–100.
[66] D. Kiener, A.M. Minor, Source truncation and exhaustion: insights from quantitative in situ TEM tensile testing, Nano Lett. 11 (2011) 3816–3820.
[67] C. Chisholm, H. Bei, M.B. Lowry, J. Oh, S.A. Syed Asif, O.L. Warren, et al., Dislocation starvation and exhaustion hardening in Mo alloy nanofibers, Acta Mater. 60 (2012) 2258–2264.
[68] A.S. Schneider, D. Kiener, C.M. Yakacki, H.J. Maier, P.A. Gruber, N. Tamura, et al., Influence of bulk pre-straining on the size effect in nickel compression pillars, Mater. Sci. Eng. A, Struct. Mater.: Prop. Microstruct. Process. 559 (2013) 147–158.
[69] D. Kiener, W. Grosinger, G. Dehm, R. Pippan, A further step towards an understanding of size-dependent crystal plasticity: In situ tension experiments of miniaturized single-crystal copper samples, Acta Mater. 56 (2008) 580–592.
[70] A.T. Jennings, J.R. Greer, Tensile deformation of electroplated copper nanopillars, Philos. Mag. 91 (2011) 1108–1120.
[71] Y. Lu, Y. Ganesan, J. Lou, A multi-step method for in situ mechanical characterization of 1-D nanostructures using a novel micromechanical device, Exp. Mech. 50 (2009) 47–54.
[72] Y. Lu, C. Peng, Y. Ganesan, J.Y. Huang, J. Lou, Quantitative in situTEM tensile testing of an individual nickel nanowire, Nanotechnology 22 (2011) 355702.
[73] Web site: G. Fried, J. Wozniak, Imaging technology group: http://itg.beckman.illinois.edu/communications/iotw/2002-08-01/, August 1, 2002.
[74] Web site: I.M. Robertson, IMR Group – Facilities, Robertson.Matse.Illinois.Edu.
[75] J.A. Sharon, Y. Zhang, F. Mompiou, M. Legros, K.J. Hemker, Discerning size effect strengthening in ultrafine-grained Mg thin films, Scr. Mater. 75 (2013) 10–13.
[76] M.A. Haque, M.T.A. Saif, Mechanical behavior of 30–50 nm thick aluminum films under uniaxial tension, Scr. Mater. 47 (2002) 863–867.
[77] J.H. Han, M.T.A. Saif, In situ microtensile stage for electromechanical characterization of nanoscale freestanding films, Rev. Sci. Instrum. 77 (2006) 045102-8.
[78] M.A. Haque, M.T.A. Saif, In situ tensile testing of nanoscale freestanding thin films inside a transmission electron microscope, J. Mater. Res. 20 (2005) 1769–1777.
[79] J. Rajagopalan, J.H. Han, T.A. Saif, Plastic deformation recovery in freestanding nanocrystalline aluminum and gold thin films, Science 315 (2007) 1831–1834.
[80] J. Rajagopalan, C. Rentenberger, H. Peter Karnthaler, G. Dehm, M.T.A. Saif, In situ TEM study of microplasticity and Bauschinger effect in nanocrystalline metals, Acta Mater. 58 (2010) 4772–4782.

[81] M.A. Haque, M.T.A. Saif, Deformation mechanisms in free-standing nanoscale thin films: A quantitative in situ transmission electron microscope study, Proc. Natl. Acad. Sci. USA 101 (2004) 6335–6340.
[82] Y. Zhu, H.D. Espinosa, An electromechanical material testing system for in situ electron microscopy and applications, Proc. Natl. Acad. Sci. USA 102 (2005) 14503–14508.
[83] H.D. Espinosa, Y. Zhu, N. Moldovan, Design and operation of a MEMS-based material testing system for nanomechanical characterization, J. Microelectromech. Syst. 16 (2007) 1219–1231.
[84] H.D. Espinosa, R.A. Bernal, T. Filleter, In Situ TEM electromechanical testing of nanowires and nanotubes, Small 8 (2012) 3233–3252.
[85] R. Agrawal, B. Peng, E.E. Gdoutos, H.D. Espinosa, Elasticity size effects in ZnO nanowires – a combined experimental-computational approach, Nano Lett. 8 (2008) 3668–3674.
[86] B. Pant, B.L. Allen, T. Zhu, K. Gall, O.N. Pierron, A versatile microelectromechanical system for nanomechanical testing, Appl. Phys. Lett. 98 (2011), 053506–053503.
[87] T. Ishida, Y. Nakajima, K. Kakushima, M. Mita, H. Toshiyoshi, H. Fujita, Design and fabrication of MEMS-controlled probes for studying the nano-interface under in situ TEM observation, J. Micromech. Microeng. 20 (2010) 075011.
[88] T. Sato, T. Ishida, L. Jalabert, H. Fujita, Real-time transmission electron microscope observation of nanofriction at a single Ag asperity, Nanotechnology 23 (2012) 505701.
[89] T. Sato, L. Jalabert, H. Fujita, Development of MEMS integrated into TEM setup to monitor shear deformation, force and stress for nanotribology, Microelectron. Eng. 112 (2013) 269–272.
[90] M. Ciappa, Selected failure mechanisms of modern power modules, Microelectron. Reliab. 42 (2002) 653–667.
[91] J. Welser, J.L. Hoyt, S. Takagi, J.F. Gibbons, Strain dependence of the performance enhancement in strained-Si n-MOSFETs, in: International Electron Devices Meeting, IEDM '94, Technical Digest., 1994, pp. 373–376.
[92] J.W. Matthews, A.E. Blakeslee, Defects in epitaxial multilayers: I. Misfit dislocations, J. Cryst. Growth 27 (1974) 118–125.
[93] J.W. Matthews, A.E. Blakeslee, Defects in epitaxial multilayers: II. Dislocation pile-ups, threading dislocations, slip lines and cracks, J. Cryst. Growth 29 (1975) 273–280.
[94] R. Hull, J.C. Bean, Variation in misfit dislocation behavior as a function of strain in the GeSi/Si system, Appl. Phys. Lett. 54 (1989) 925–927.
[95] M.J. Hytch, F. Houdellier, F. Hüe, E. Snoeck, Nanoscale holographic interferometry for strain measurements in electronic devices, Nature 453 (2008) 1086–1089.
[96] W.D. Nix, Mechanical properties of thin films, Metall. Trans. A 20A (1989) 2217–2245.
[97] W.D. Nix, Yielding and strain hardening of thin metal films on substrates, Scr. Mater. 39 (1998) 545–554.
[98] P.A. Flinn, D.S. Gardner, W.D. Nix, Measurements and interpretation of stress in aluminum-based metallization as a function of thermal history, IEEE Trans. Electron Devices 34 (1987) 689–699.
[99] P.A. Flinn, Measurements and interpretation of stress in copper films as a function of thermal history, J. Mater. Res. 6 (1991) 1498–1501.
[100] G. Wiederhirn, The strength limits of ultra-thin copper films, Ph.D. dissert., University of Stuttgart, Germany, 2007.
[101] P. Müllner, E. Arzt, Observation of dislocation disappearance in aluminum thin films and consequences for thin film properties, in: Mater. Res. Soc., Warrendale, PA, Boston, MA, 1998, p. 149.
[102] M. Legros, G. Dehm, R.M. Keller-Flaig, E. Arzt, K.J. Hemker, S. Suresh, Dynamic observation of Al thin films plastically strained in a TEM, Mater. Sci. Eng. A, Struct. Mater.: Prop. Microstruct. Process. 309–310 (2001) 463–467.
[103] R.M. Keller, W. Sigle, S.P. Baker, O. Kraft, E. Arzt, In situ TEM investigation during thermal cycling of thin copper films, in: S.P. Baker, J. Gao, W.W. Gerberich, J.-E. Sundgren (Eds.), Thin Films Stresses and Mechanical Properties VI, MRS Proc. 436 (1996).
[104] R.M. Keller, S.P. Baker, E. Arzt, Quantitative analysis of strengthening mechanisms in thin Cu films: Effects of film thickness, grain size, and passivation, J. Mater. Res. 13 (1998) 1307–1317.
[105] R.M. Keller-Flaig, M. Legros, W. Sigle, A. Gouldstone, K.J. Hemker, S. Suresh, et al., In situ transmission electron microscopy investigation of threading dislocation motion in passivated thin aluminum films, J. Mater. Res. 14 (1999) 4673–4676.
[106] M. Legros, Small-scale plasticity, in: Mechanics of Nano-Objects, École des Mines de Paris Éditions, Paris, 2011.
[107] M. Legros, Relaxation plastique des couches métalliques par dislocations et défauts étendus, in: Contraintes mécaniques en micro, nano Et optoélectronique (Traité EGEM, Série Électronique Et Micro-Électronique), Hermes Science Publications, Paris, 2006.
[108] B.J. Inkson, G. Dehm, T. Wagner, In situ TEM observation of dislocation motion in thermally strained Al nanowires, Acta Mater. 50 (2002) 5033–5047.
[109] M. Legros, G. Dehm, T.J. Balk, In situ TEM study of plastic stress relaxation mechanisms and interface effects in metallic films, in: T. Buchheit, A. Minor, R. Spolenak, K. Takashima (Eds.), Thin Films – Stresses and Mechanical Properties XI, MRS Proc. 875 San Francisco (2005) 237–247.
[110] G. Dehm, T.J. Balk, H. EdonguÈ, E. Arzt, Small-scale plasticity in thin Cu and Al films, Microelectron. Eng. 70 (2003) 412–424.
[111] T.J. Balk, G. Dehm, E. Arzt, Parallel glide: unexpected dislocation motion parallel to the substrate in ultrathin copper films, Acta Mater. 51 (2003) 4471–4485.
[112] H. Gao, A. Hartmaier, M.J. Buehler, A discrete dislocation plasticity model of creep in polycrystalline thin films, Defect Diffus. Forum (2003) 107–126, 224-225.
[113] M.J. Buehler, A. Hartmaier, H. Gao, Atomistic and continuum studies of crack-like diffusion wedges and associated dislocation mechanisms in thin films on substrates, J. Mech. Phys. Solids 51 (2003) 2105–2125.
[114] J.P. Hirth, L. J, Theory of Dislocations, 2nd ed., John Wiley and Sons, New York, 1982.
[115] J. Friedel, Dislocations, in: Dislocations, Pergamon Press, Oxford, 1967, pp. 45–46.
[116] F. Mompiou, M. Legros, Plasticity mechanisms in sub-micron Al fiber investigated by in situ TEM, Adv. Eng. Mater. 14 (2012) 955–959.
[117] D. Caillard, On the stress discrepancy at low-temperatures in pure iron, Acta Mater. 62 (2014) 267–275.
[118] F. Mompiou, D. Caillard, M. Legros, H. Mughrabi, In situ TEM observations of reverse dislocation motion upon unloading in tensile-deformed UFG aluminium, Acta Mater. 60 (2012) 3402–3414.
[119] S. Farenc, D. Caillard, A. Couret, An in situ study of prismatic glide in α titanium at low temperatures, Acta Metall. Mater. 41 (1993) 2701–2709.
[120] M. Legros, A. Couret, D. Caillard, Prismatic and basal slip in Ti3Al. II. Dislocation interactions and cross-slip processes, Philos. Mag. A 73 (1996) 81–99.
[121] S. Zghal, A. Menand, A. Couret, Pinning points anchoring ordinary and Shockley dislocations in TiAl alloys, Acta Mater. 46 (1998) 5899–5905.
[122] P. Castany, F. Pettinari-Sturmel, J. Crestou, J. Douin, Experimental study of dislocation mobility in a Ti–6Al–4V alloy, Acta Mater. 18 (2007) 6284–6291.
[123] J. Douin, F. Pettinari-Sturmel, A. Coujou, Dissociated dislocations in confined plasticity, Acta Mater. 55 (2007) 6453–6458.
[124] D. Caillard, J.L. Martin, Thermally Activated Mechanisms in Crystal Plasticity, Pergamon Press, Cambridge, 2003.
[125] M. Legros, G. Dehm, E. Arzt, T.J. Balk, Observation of giant diffusivity along dislocation cores, Science 319 (2008) 1646–1649.
[126] F. Pettinari-Sturmel, G. Saada, J. Douin, A. Coujou, N. Clément, Quantitative analysis of dislocation pile-ups in thin foils compared to bulk, Mater. Sci. Eng. A, Struct. Mater.: Prop. Microstruct. Process. 387–389 (2004) 109–114.
[127] M. Chassagne, M. Legros, D. Rodney, Atomic-scale simulation of screw dislocation/coherent twin boundary interaction in Al, Au, Cu and Ni, Acta Mater. 59 (2011) 1456–1463.
[128] G. Saada, J. Douin, F. Pettinari-Sturmel, A. Coujou, N. Clément, Pile-ups in thin foils: application to transmission electron microscopy analysis of short-range-order, Philos. Mag. 84 (2006) 807–824.

[129] B. Pan, B. Pan, K. Qian, K. Qian, H. Xie, H. Xie, et al., Two-dimensional digital image correlation for in-plane displacement and strain measurement: a review, Meas. Sci. Technol. 20 (2009) 062001.
[130] C. Eberl, D.S. Gianola, R. Thompson, Digital Image Correlation and Tracking, The Mathworks, Inc., 2006.
[131] D. Gianola, M. Legros, K.J. Hemker, W.J. Sharpe, Experimental techniques for uncovering deformation mechanisms in nanocrystalline Al thin films, TMS Lett. (2004) 149–150.
[132] D.S. Gianola, A. Sedlmayr, R. Mönig, C.A. Volkert, R.C. Major, E. Cyrankowski, et al., In situ nanomechanical testing in focused ion beam and scanning electron microscopes, Rev. Sci. Instrum. 82 (2011) 063901–063912.
[133] F. Mompiou, D. Caillard, M. Legros, Grain-boundary mediated plasticity in nanocrystalline Al films, in: Materials Research Society Proceedings, San Francisco, 2008.
[134] F. Mompiou, M. Legros, D. Caillard, Direct observation and quantification of grain boundary shear-migration coupling in polycrystalline Al, J. Mater. Sci. 46 (2011) 4308–4313.
[135] F. Mompiou, D. Caillard, M. Legros, Grain boundary shear-migration coupling–I. In situ TEM straining experiments in Al polycrystals, Acta Mater. 57 (2009) 2198–2209.
[136] J.W. Cahn, J.E. Taylor, A unified approach to motion of grain boundaries, relative tangential translation along grain boundaries, and grain rotation, Acta Mater. 52 (2004) 4887–4898.
[137] J.W. Cahn, Y. Mishin, A. Suzuki, Coupling grain boundary motion to shear deformation, Acta Mater. 54 (2006) 4953–4975.
[138] A. Rajabzadeh, F. Mompiou, M. Legros, N. Combe, Elementary mechanisms of shear-coupled grain boundary migration, Phys. Rev. Lett. (2013) 265507.
[139] G. Gottstein, D.A. Molodov, L.S. Shvindlerman, D.J. Srolovitz, M. Winning, Grain boundary migration: misorientation dependence, Curr. Opin. Solid State Mater. Sci. 5 (2001) 9.
[140] A. Rajabzadeh, M. Legros, N. Combe, Evidence of grain boundary dislocation step motion associated to shear-coupled grain boundary migration, Philos. Mag. 93 (2013) 1299–1316.
[141] D. Caillard, F. Mompiou, M. Legros, Grain-boundary shear-migration coupling. II: Geometrical model for general boundaries, Acta Mater. 57 (2009) 2390–2402.
[142] M. Kim, J.M. Zuo, G.-S. Park, High-resolution strain measurement in shallow trench isolation structures using dynamic electron diffraction, Appl. Phys. Lett. 84 (2004) 2181–2183.
[143] M. Legros, O. Ferry, F. Houdellier, A. Jacques, A. George, Fatigue of single crystalline silicon: Mechanical behaviour and TEM observations, Mater. Sci. Eng. A, Struct. Mater.: Prop. Microstruct. Process. 483–484 (2008) 353–364.
[144] M.J. Hytch, J.L. Putaux, J.M. Pénisson, Measurement of the displacement field of dislocations to 0.03 A by electron microscopy, Nature 425 (2003) 270–273.
[145] F. Hüe, M. Hÿtch, H. Bender, F. Houdellier, A. Claverie, Direct mapping of strain in a strained silicon transistor by high-resolution electron microscopy, Phys. Rev. Lett. 100 (2008) 156602.
[146] M. Legros, F. Houdellier, M. Martinez, A. Danilov, L. De Knoop, M. Hÿtch, *In Situ* dark field electron holography with a double tilt nano-indentation holder, in: International Microscopy Congress, Rio de Janeiro, 2010.
[147] Web site, K. Ishizuka, GPA for DigitalMicrograph, www.hremresearch.com.
[148] E.A. Stach, D. Zakharov, R.D. Rivas, P. Longo, M. Lent, A. Gubbens, et al., Exploiting a direct detection camera for in situ microscopy, Microsc. Microanal. 19 (2013) 392–393.